



ELSEVIER

Available online at www.sciencedirect.com



International Journal of Thermal Sciences 42 (2003) 749–757

International
Journal of
Thermal
Sciences

www.elsevier.com/locate/ijts

Non-uniform multiple slot injection (suction) or wall enthalpy into a compressible flow over a yawed circular cylinder

S.V. Subhashini^a, H.S. Takhar^{b,*}, G. Nath^c

^a Department of Mathematics, S.R.M. Engineering College, S.R.M. Nagar, Kancheepuram District, Tamilnadu 603203, India

^b Department of Engineering, Manchester Metropolitan University, Manchester M1 5GD, UK

^c Department of Mathematics, Indian Institute of Science, Bangalore 560012, India

Received 6 June 2002; accepted 24 October 2002

Abstract

Steady non-similar laminar compressible boundary layer flows over yawed infinite cylinder with non-uniform multiple slot injection/suction and non-uniform wall enthalpy have been studied. The numerical difficulties are overcome by applying the method of quasi-linear implicit finite difference scheme with an appropriate selection of finer stepsize along the streamwise direction. Separation can be delayed more effectively by non-uniform multiple slot suction and also by moving the slots downstream as compared to the non-uniform single slot suction but the non-uniform multiple slot injection has the reverse effect. Increase of Mach number shifts the point of separation upstream due to the increase in the adverse pressure gradient. An increase of enthalpy at the wall causes separation to occur earlier while cooling delays it. Non-uniform total enthalpy at the wall has very little effect on the skin frictions or the point of separation. Also, the yaw angle has very little effect on the location of the point of separation.

© 2003 Éditions scientifiques et médicales Elsevier SAS. All rights reserved.

Keywords: Compressible boundary layers and multiple slot injection; Suction

1. Introduction

The existence of cross flow which occurs in the boundary layer of an yawed cylinder is important for understanding the aerodynamic properties of swept wings. Studies on yawed cylinder boundary layer have a practical interest also. When yawed or swept back wings operate at higher lift, the pressure on the suction side near the leading edge shows a considerable gradient towards the receding tip, caused by the rearward shift of the aero-foil sections of the wing. The decelerated fluid particles in the boundary layer have a tendency to travel in the direction of this gradient and a cross flow in the direction of the receding tip producing a detrimental effect on the aerodynamic properties of the wing. A detailed survey of the literature on flow past a yawed infinite cylinder has been made by Dewey and Gross [1] but in most past studies, the solutions of non-similar flows have been obtained by using approximate methods such as the momentum integral, series expansion, local similarity, the

local non-similarity, etc. and the exact location of the point of separation was not reached. But it is of more practical use to obtain exact solutions of non-similar flows using advanced numerical techniques and the accurate prediction of the point of separation may be helpful in reducing the energy losses due to the formation of boundary layer and its separation.

The nature of steady three-dimensional laminar boundary layer separation may be characterized by two possible modes: singular separation and ordinary separation, which has been pointed out by Maskell [2]. For the singular separation, both (longitudinal and transverse) components of the wall shear vanish simultaneously and for the ordinary separation, only one component (longitudinal) of the wall shear vanishes. Cebeci et al. [3] and Smith [4] have given excellent reviews on boundary layer separation phenomenon. It is noted that in both the incompressible and compressible flow cases, due to separation of the boundary layer, there is a decrease in the pressure and consequently a sharp increase in drag and decrease in lift. To overcome this disadvantage, it is desired to at least partially delay the separation. There are two mechanisms widely used to control the boundary layer

* Corresponding author.

E-mail address: h.s.takhar@mmu.ac.uk (H.S. Takhar).

Nomenclature

A	mass transfer parameter
C_f, \bar{C}_f	skin friction co-efficients in the x, z -directions
C_p	specific heat at constant pressure ... $\text{kJ}\cdot\text{kg}^{-1}\cdot\text{K}$
E	dissipation parameter
f	dimensionless stream function
F	dimensionless chordwise velocity
G	dimensionless total enthalpy
h, H	specific and total enthalpy
K	thermal conductivity $\text{W}\cdot\text{m}^{-1}\cdot\text{K}$
L	characteristic length m
M	Mach number
N	Chapman–Rubesin function
Nu	Nusselt number
P	pressure Pa
Pr	Prandtl number
q_w	rate of heat transfer at the wall
Re	Reynolds number
S	dimensionless spanwise velocity
T	temperature K
u, v, w	velocity components in the x, y, z -directions $\text{m}\cdot\text{s}^{-1}$
U_∞	resultant freestream velocity
x, y, z	dimensional chordwise, normal to the surface and spanwise distances, respectively m

\bar{x}	$= x/R$, dimensionless chordwise distance
\bar{x}_1, \bar{x}_2	slot locations parameter

Greek symbols

β	Pressure gradient function
η, ξ	dimensionless similarity variables
θ	yaw angle
ε	small parameter
$\Delta\eta, \Delta\bar{x}$	stepsizes in the η, \bar{x} -directions
μ	dynamic viscosity $\text{kg}\cdot\text{m}^{-1}\cdot\text{s}^{-1}$
ν	kinematic viscosity $\text{m}^2\cdot\text{s}^{-1}$
ρ	density $\text{kg}\cdot\text{m}^{-3}$
ψ	stream function $\text{m}^2\cdot\text{s}^{-1}$
ω^*	slot length parameter

Subscripts

∞	conditions in the free stream
e, w	denote conditions at the edge of the boundary layer and on the surface, respectively
x, y, z	partial derivatives with respect to x, y, z , respectively
η, ξ	partial derivatives with respect to η, ξ , respectively

separation, namely, suction and injection [5–7]. Fluid injection/suction is widely used in the aircraft for reducing heat transfer across turbine blades and is an effective means of controlling transition and/or separation of boundary layers over airplane control surfaces.

Mass transfer through wall slot (i.e., mass transfer occurs in small porous sections of the body surface and there is no mass transfer in the remaining part of the body surface) into the boundary layer is of interest for various potential applications including thermal protection, fuel injection in ramjet engines, energizing of the inner portion of boundary layers in adverse pressure gradients, and skin friction reduction on high speed aircraft. References [8–12] present different studies on the effect of slot injection/suction into a laminar compressible boundary layer over a flat plate. In recent investigations, Roy and Nath [13], and Roy [14] have studied the effects of non-uniform single slot injection/suction and non-uniform total enthalpy at the wall into steady non-similar compressible boundary layer flows over two-dimensional and axi-symmetric bodies, and over yawed circular cylinder. In both the above studies [13,14], non-uniform injection and suction combinations have been used in a single slot to study the effect of non-uniform mass transfer.

The aim of this investigation is to study the effects of non-uniform multiple slot injection/suction and non-uniform total enthalpy at the wall (wall cooling or heating takes place in the slots and the remaining part of the body surface has

a constant value of the total enthalpy) on the steady non-similar compressible boundary layer flow over yawed cylinder, which has not yet been studied by earlier investigators. Compressible boundary layer flow over yawed cylinder provides many practical applications. For example, the yawed infinite cylinder simulates approximately the leading edge of a swept-back wing or a body of high fineness ratio at an angle of attack and also allows a basic simplification of the complicated three-dimensional compressible boundary layer equations. Thus, the study of the effects of non-uniform multiple slot injection/suction and non-uniform wall enthalpy on a steady non-similar laminar compressible boundary layer flow over yawed infinite cylinder are useful in understanding many boundary layer problems of practical importance. Uniform mass transfer in the slots or uniform heating (or cooling) in the slots causes finite discontinuity at the leading and trailing edges of the slots. Hence, the mass transfer or the wall temperature distributions are chosen in such a way that there is no discontinuity.

The non-similar solutions have been obtained starting from the origin of the streamwise co-ordinate to the point of separation for non-uniform multiple slot injection (suction) or non-uniform wall enthalpy. The computational difficulties encountered at the origin of the streamwise co-ordinate, at the edges of the slots and near the point of separation have been overcome by using the quasi-linearization technique with an implicit finite difference scheme. There are two

types of free parameters in this problem, one type of parameters measures the length of the slots and another type of parameters fixes the position of the slots. These two sets of parameters vary the lengths and locations of the slots, respectively.

It may be noted that in our analysis the discontinuities at the leading and trailing edges of the slots have been avoided following [13,14]. Thus the present analysis differs from those in [8–12] with finite discontinuities.

2. Basic equations and transformations

Consider a boundary layer flow over a yawed infinite cylinder placed in uniform compressible flow of velocity U_∞ having components u_∞ , w_∞ and v_∞ , in the chordwise, spanwise and in the orthogonal direction to the surface, respectively. The distances in respective directions are designated as x , z and y as shown in Fig. 1. The blowing rate is assumed to be small and it does not affect the inviscid flow at the edge of the boundary layer. The inviscid (potential) flow is considered to be isentropic. It is also assumed that the injected fluid possesses the same physical properties as the boundary layer fluid and has a static temperature equal to the wall temperature. Both fluids are assumed to be perfect fluids. The Prandtl number Pr is assumed to be constant as its variation across the boundary layer is negligible for most of the atmospheric problems [15]. It was shown by Cambel [16] that the specific heat of argon plasma is constant at constant pressure if the temperature is less than 10,000 K. It was also shown that the viscosity μ and the thermal conductivity K vary linearly with temperature in that range. Schlichting [17] has also shown for gases that the viscosity and the thermal conductivity vary in the same way with temperature (see Table 12.1 of Schlichting [17]). Therefore the local Prandtl number Pr remains nearly constant. It is

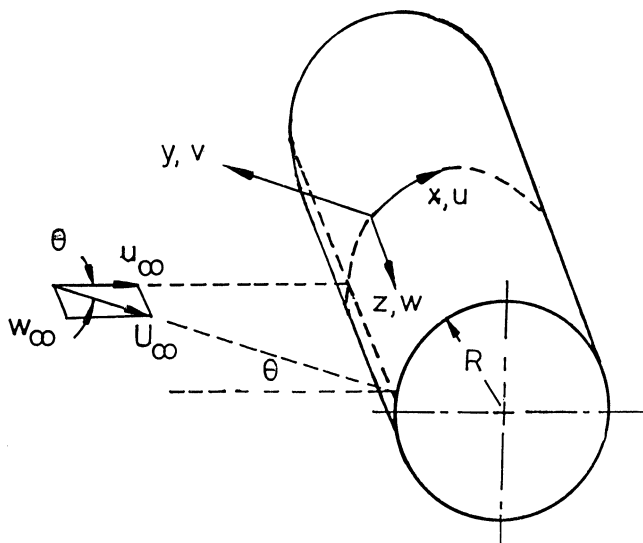


Fig. 1. Flow model and co-ordinate system.

assumed that the potential flow depends on x , but not on z , i.e., when $u_e = u_e(x)$, $w_e = w_e(x)$. Hence the boundary layer equations will be independent of z . Under the foregoing assumptions, the boundary layer equations governing the steady laminar compressible flow are [17,18]:

Continuity:

$$(\rho u)_x + (\rho v)_y = 0 \tag{1}$$

Momentum:

$$\rho[uu_x + vu_y] = -P_x + (\mu u_y)_y \tag{2}$$

$$\rho[uw_x + vw_y] = -P_z + (\mu w_y)_y \tag{3}$$

Energy:

$$\rho[uH_x + vH_y] = \left(\frac{\mu}{Pr} H_y\right)_y + [\mu(1 - Pr^{-1})(uu_y + ww_y)]_y \tag{4}$$

where

$$-P_x = \rho_e u_e (u_e)_x \quad \text{and} \quad -P_z = \rho_e u_e (w_e)_x \tag{5}$$

The boundary conditions are given by

$$\begin{aligned} u(x, 0) = 0, \quad v(x, 0) = v_w(x) \\ w(x, 0) = 0, \quad H(x, 0) = H_w(x) \end{aligned} \tag{6}$$

$$\begin{aligned} u(x, \infty) = u_e(x), \quad v(x, \infty) = 0 \\ w(x, \infty) = w_e, \quad H(x, \infty) = H_e \end{aligned} \tag{7}$$

where the total enthalpy H can be written as $H = h + 1/2(u^2 + w^2) = C_p T + 1/2(u^2 + w^2)$. The total enthalpy at the edge of the boundary layer $H_e = \text{constant}$, since the potential flow is isentropic. Here ρ and P are the density and pressure, respectively. The subscripts x , y , z denote partial derivatives with respect to those variables. Further, the subscripts w and e denote conditions at the wall and at the edge of the boundary layer, respectively; h and C_p are, respectively, the static enthalpy and the specific heat at constant pressure; $v_w(x)$ denotes the surface mass transfer.

Applying the following transformations:

$$\begin{aligned} \xi = \int_0^x \rho_e \mu_e u_e dx, \quad \eta = u_e (2\xi)^{-1/2} \int_0^y \rho dy \\ f(\xi, \eta) = (2\xi)^{-1/2} \psi(x, y), \quad \rho u = \frac{\partial \psi}{\partial y}, \quad \rho v = -\frac{\partial \psi}{\partial x} \\ u = u_e f_\eta(\xi, \eta) = u_e F(\xi, \eta), \quad w = w_e S(\xi, \eta) \\ H = H_e G(\xi, \eta), \quad H_e = H_\infty \end{aligned} \tag{8}$$

to Eqs. (1)–(4), we find that Eq. (1) is identically satisfied and Eqs. (2)–(4) reduce to non-dimensional form given by

$$\begin{aligned} (NF_\eta)_\eta + fF_\eta + \beta(\xi) \{(\rho_e/\rho) - F^2\} \\ = 2\xi(FF_\xi - F_\eta f_\xi) \end{aligned} \tag{9}$$

$$(NS_\eta)_\eta + fS_\eta = 2\xi(FS_\xi - S_\eta f_\xi) \tag{10}$$

$$(NG_\eta)_\eta + Pr f G_\eta - 2(1 - Pr)E \times [NFF_\eta(u_e/u_\infty)^2 \cos^2 \theta + NSS_\eta \sin^2 \theta]_\eta = 2\xi(FG_\xi - G_\eta f_\xi) \tag{11}$$

Here ξ and η are transformed co-ordinates, ψ and f are the dimensional and dimensionless stream functions, respectively; S and G are respectively, the dimensionless spanwise velocity and total enthalpy; the subscripts ξ and η denote the partial derivatives with respect to those variables. Here N is the Chapman–Rubesin function, $\beta(\xi)$ and E are the pressure gradient and dissipation (Eckert number) parameters, respectively, given by

$$N = \frac{\rho\mu}{\rho_e\mu_e}, \quad \beta = \frac{2\xi}{u_e} \frac{du_e}{d\xi}$$

$$E = \frac{U_\infty^2}{2H_e} = \frac{(\gamma - 1)M_\infty^2}{2 + (\gamma - 1)M_\infty^2}$$

where U_∞ , M_∞ and γ ($= 1.4$ for air) are, respectively, the resultant freestream velocity, the freestream Mach number and the ratio of specific heats. The transformed boundary conditions are

$$F(\xi, 0) = 0, \quad S(\xi, 0) = 0, \quad G(\xi, 0) = G_w P(\bar{x})$$

$$F(\xi, \infty) = 1, \quad S(\xi, \infty) = 1, \quad G(\xi, \infty) = 1 \tag{12}$$

where $G_w P(\bar{x})$ is the total enthalpy distribution prescribed at the wall and

$$f = \int_0^\eta F d\eta + f_w,$$

$$f_w = - \left[2\xi f_\xi(\xi, 0) + (\rho v)_w (2\xi)^{1/2} \left(\frac{d\xi}{dx} \right)^{-1} \right]$$

From the above equation, f_w can be written as

$$f_w = -(2\xi)^{-1/2} \int_0^x (\rho v)_w dx \tag{13}$$

It may be noted that the system of Eqs. (9)–(11) reduces to that of two-dimensional case for $\theta = 0$. Hence Eq. (10) becomes redundant as the velocity component in the z -direction $w = 0$ (i.e., $S = 0$) for $\theta = 0$.

The potential flow velocity for a yawed finite circular cylinder of radius R in subsonic flow is given by [19].

$$u_e(\bar{x}) = u_\infty (A_1 \sin \bar{x} + A_2 \sin 3\bar{x})$$

$$w_e = w_\infty = \text{constant} \tag{14}$$

where $A_1 = 2(1 + M_\infty^2/3)$, $A_2 = -M_\infty^2/2$, $\bar{x} = x/R$. It may be remarked that in Eq. (14), which is valid for subsonic flow ($M_\infty \leq 0.4$), we have retained the terms up to order (M_∞^2) only. If the terms up to the next order i.e., up to order (M_∞^4) are included in the series (14), the flow on the surface of the cylinder at $\bar{x} = \pm\pi/2$ becomes locally supersonic [20] at $M_\infty \approx 0.404$. For $0.404 < M_\infty < 0.45$, there are regions just above and just below the cylinder in which the flow

is supersonic and there is an apparently smooth transition from subsonic flow elsewhere. For $M_\infty > 0.45$, the series (14) appears to diverge [20]. Experimentally it has been found that local shock waves appear for about $M_\infty = 0.45$. Consequently, as a first step, we have investigated only the subsonic flow ($M_\infty \leq 0.4$), because several investigators encountered considerable difficulty both at the origin and near the point of separation. The analogous supersonic or hypersonic case will be considered separately as the potential flow solution has to be obtained numerically before proceeding to the boundary layer solution.

Using the relation (14), the expressions for ξ , β and f_w can be written as

$$\xi = R\rho_e\mu_e u_\infty P_3, \quad \beta = 2 \cos \bar{x} P_4 P_5 P_2^{-1} P_6^{-2} \tag{15}$$

$$f_w = 0 \quad \text{for } \bar{x} \leq \bar{x}_1$$

$$= A(\cos \theta)^{-1/2} P_3^{-1/2} C(\bar{x}, \bar{x}_1) \quad \text{for } \bar{x}_1 \leq \bar{x} \leq \bar{x}_1^*$$

$$= A(\cos \theta)^{-1/2} P_3^{-1/2} C(\bar{x}_1^*, \bar{x}_1) \quad \text{for } \bar{x}_1^* \leq \bar{x} \leq \bar{x}_2$$

$$= A(\cos \theta)^{-1/2} P_3^{-1/2} C(\bar{x}_1^*, \bar{x}_1)$$

$$+ A(\cos \theta)^{-1/2} P_3^{-1/2} C(\bar{x}, \bar{x}_2) \quad \text{for } \bar{x}_2 \leq \bar{x} \leq \bar{x}_2^*$$

$$= A(\cos \theta)^{-1/2} P_3^{-1/2} C(\bar{x}_1^*, \bar{x}_1)$$

$$+ A(\cos \theta)^{-1/2} P_3^{-1/2} C(\bar{x}_2^*, \bar{x}_2) \quad \text{for } \bar{x} \geq \bar{x}_2^* \tag{16}$$

where the function $C(s, t)$ is given by

$$C(s, t) = 1 - \cos\{\omega^*(s - t)\}$$

and

$$P_1 = 1 - \cos \bar{x}, \quad P_2 = 1 + \cos \bar{x}$$

$$P_3 = A_1 P_1 + A_2 (1 - \cos 3\bar{x})/3$$

$$P_4 = A_1 + 3A_2 (4 \cos^2 \bar{x} - 3)$$

$$P_5 = A_1 + A_2 (1 + 4P_2 \cos \bar{x})/3$$

$$P_6 = A_1 + A_2 (3 - 4 \sin^2 \bar{x})$$

Here $(\rho v)_w$ is taken as

$$(\rho v)_w = -(\rho_e U_\infty)(Re/2)^{-1/2} A \omega^* \sin\{\omega^*(\bar{x} - \bar{x}_1)\}$$

$$\text{for } \bar{x}_1 \leq \bar{x} \leq \bar{x}_1^*$$

$$= -(\rho_e U_\infty)(Re/2)^{-1/2} A \omega^* \sin\{\omega^*(\bar{x} - \bar{x}_2)\}$$

$$\text{for } \bar{x}_2 \leq \bar{x} \leq \bar{x}_2^*$$

$$= 0 \quad \text{for } \bar{x} \leq \bar{x}_1, \bar{x}_1^* \leq \bar{x} \leq \bar{x}_2 \text{ or } \bar{x} \geq \bar{x}_2^* \tag{17}$$

where $Re = (U_\infty R/\nu_e)$, and ω^* and $(\bar{x}_1, \bar{x}_2; \bar{x}_1 < \bar{x}_2)$ are two sets of free parameters which, respectively, determine the lengths and locations of the slots. The subscripts ‘1’ and ‘2’ denote for first and second slot, respectively. The function $(\rho v)_w$ is continuous for all values for \bar{x} and it has non-zero values only in the intervals (\bar{x}_1, \bar{x}_1^*) and (\bar{x}_2, \bar{x}_2^*) . The reason for taking such a type of function is that it allows the mass transfer to change slowly in the neighbourhood of the leading and trailing edges of the slots. The parameter $A > 0$ or $A < 0$ is taken according to whether there is a suction or injection. Since the flow considered here is a

subsonic one, it is reasonable to take the fluid medium as one, which has constant gas properties. Accordingly, we have

$$\rho \propto h^{-1}, \quad \mu \propto h, \quad Pr = \text{constant}$$

and

$$\frac{\rho_e}{\rho} = \frac{G - E\{(u_e/u_\infty)^2 \cos^2 \theta F^2 + \sin^2 \theta S^2\}}{1 - E\{(u_e/u_\infty)^2 \cos^2 \theta + \sin^2 \theta\}} \quad (18)$$

It is convenient to express Eqs. (9)–(11) in terms \bar{x} instead of ξ . Eq. (15) gives the relation between ξ and \bar{x} as

$$\xi \frac{\partial}{\partial \xi} = B(\bar{x}) \frac{\partial}{\partial \bar{x}} \quad (19)$$

where $B(\bar{x})$ is given by

$$B(\bar{x}) = P_3 P_6^{-1} / (\sin \bar{x})$$

Substituting Eqs. (18) and (19) in Eqs. (9)–(11), we obtain

$$F_{\eta\eta} + f F_\eta + \beta_1 [G - F^2 + E_1 (F^2 - S^2)] = 2B(\bar{x})(F F_{\bar{x}} - F_\eta f_{\bar{x}}) \quad (20)$$

$$S_{\eta\eta} + f S_\eta = 2B(\bar{x})(F S_{\bar{x}} - S_\eta f_{\bar{x}}) \quad (21)$$

$$G_{\eta\eta} + Pr f G_\eta - 2(1 - Pr) \times [E_2 F F_{\eta\eta} + E_2 F_\eta^2 + E_1 S S_{\eta\eta} + E_1 S_\eta^2] = 2PrB(\bar{x})(F G_{\bar{x}} - G_\eta f_{\bar{x}}) \quad (22)$$

where $E_1 = E \sin^2 \theta$, $E_2 = E(u_e/u_\infty)^2 \cos^2 \theta$ and $\beta_1 = \beta / [1 - E_1 - E_2]$.

The boundary conditions become

$$F(\bar{x}, 0) = 0, \quad S(\bar{x}, 0) = 0, \quad G(\bar{x}, 0) = G_w P(\bar{x}) \\ F(\bar{x}, \infty) = 1, \quad S(\bar{x}, \infty) = 1, \quad G(\bar{x}, \infty) = 1 \quad (23)$$

where $f = \int_0^\eta F d\eta + f_w$ and f_w is given by Eq. (16). The arbitrary function $P(\bar{x})$, associated with the non-uniformity of the total enthalpy at the wall, is given by

$$P(\bar{x}) = 1 + \varepsilon \sin[\omega^*(\bar{x} - \bar{x}_1)], \quad \text{for } \bar{x}_1 \leq \bar{x} \leq \bar{x}_1^* \\ = 1 + \varepsilon \sin[\omega^*(\bar{x} - \bar{x}_2)], \quad \text{for } \bar{x}_2 \leq \bar{x} \leq \bar{x}_2^* \\ = 1, \quad \text{for } \bar{x} \leq \bar{x}_1, \bar{x}_1^* \leq \bar{x} \leq \bar{x}_2 \text{ or } \bar{x} \geq \bar{x}_2^*$$

where ε is a small real number. Here $P(\bar{x})$ is a continuous function with a small perturbation in the intervals $[\bar{x}_1, \bar{x}_1^*]$ and $[\bar{x}_2, \bar{x}_2^*]$ over the constant value ‘1’ and it gives the variation of the total enthalpy at the wall only in the intervals $[\bar{x}_1, \bar{x}_1^*]$ and $[\bar{x}_2, \bar{x}_2^*]$ while the remaining part of the body surface is maintained at the constant value of the total enthalpy at the wall (G_w). The sudden rise or fall of the total enthalpy at the edges of the slots can cause numerical difficulties in the solution of the energy equation. To avoid these, we use this type of function so that it allows the total enthalpy at the wall to change slowly in the neighbourhoods of the leading and trailing edges of the slots. It can be seen from the boundary conditions (23) that in the first slot, the distribution of the total enthalpy at the wall, given by $G_w[1 + \varepsilon \sin\{\omega^*(\bar{x} - \bar{x}_1^*)\}]$, has a constant value G_w before

the leading edge of the first slot (i.e., $0 \leq \bar{x} \leq \bar{x}_1$) and as the slot starts, total enthalpy at the wall slowly decreases (increases) and reaches its minimum (maximum) value from which it again increases (decreases) up to the constant value G_w at the trailing edge of the first slot. The distribution of total enthalpy at the wall has also similar variation in the second slot (i.e., in $\bar{x}_2 \leq \bar{x} \leq \bar{x}_2^*$). This type of function has been considered in references [13,14,21] for the variation of the wall temperature distribution in the single slot along streamwise direction.

The skin friction co-efficients in x - and z -directions (i.e., in the chordwise and spanwise directions) can be expressed in the form

$$C_f(Re)^{1/2} = 2^{1/2}(\cos \theta)^{1/2} \sin \bar{x} P_2^{1/2} P_5^{-1/2} P_6^2 (F_\eta)_w \quad (24)$$

and

$$\bar{C}_f(Re)^{1/2} = 2^{1/2}(\cos \theta)^{1/2} \sin \theta P_2^{1/2} P_5^{-1/2} P_6 (S_\eta)_w \quad (25)$$

Similarly, the heat transfer co-efficients in terms of Stanton number is defined by

$$St(Re)^{1/2} = 2^{1/2} [Pr(1 - G_w)]^{-1} \times (\cos \theta)^{1/2} P_2^{1/2} P_5^{-1/2} P_6 (G_\eta)_w \quad (26)$$

where

$$C_f = 2 \left[\mu \frac{\partial u}{\partial y} \right]_w / \rho_e U_\infty^2, \quad \bar{C}_f = 2 \left[\mu \frac{\partial w}{\partial y} \right]_w / \rho_e U_\infty^2$$

and

$$St = K / C_p \left(\frac{\partial H}{\partial y} \right)_w / [\rho_e (H_e - H_w) U_\infty]$$

Thus, it is clear from Eqs. (24)–(26) that $(F_\eta)_w$, $(S_\eta)_w$ and $(G_\eta)_w$ are the crucial parameters which characterize skin friction and heat transfer of the fluid flow.

3. Results and discussions

Eqs. (20)–(22) under the boundary conditions (23) have been solved numerically using an implicit finite difference scheme in combination with the quasi-linearization method. Since the method is described in complete detail in [22], its detailed description is not presented here. However, for the sake of completeness, its outline is given here. The non-linear coupled partial differential equations (20)–(22) were first linearized using quasi-linearization technique [22]. The resulting linear partial differential equations were expressed in difference form. The equations were then reduced to a system of linear algebraic equations with a block tri-diagonal structure, which is solved using Varga’s algorithm [23]. The stepsize in the η -direction has been chosen as $\Delta \eta = 0.01$ throughout the computation. In the \bar{x} -direction, $\Delta \bar{x} = 0.01$ has been used for small values of \bar{x} (≤ 0.50), then it has been decreased to $\Delta \bar{x} = 0.001$. This value of $\Delta \bar{x}$ has been used for $\bar{x} \leq 1.25$, thereafter the stepsize $\Delta \bar{x}$ has been reduced further, ultimately choosing a value

$\Delta\bar{x} = 0.0001$ in the neighbourhood of the point of zero skin friction. This has been done because the convergence becomes slower when the point of vanishing skin friction in chordwise direction is approached. The choice of stepsizes has been found to be optimum since further reduction does not alter the results up to the fourth decimal place.

The computations have been carried out for various values of A ($-0.5 \leq A \leq 0.5$), \bar{x}_1, \bar{x}_2 ($0.25 \leq \bar{x}_1, \bar{x}_2 \leq 1.5$), M_∞ ($0.2 \leq M_\infty \leq 0.4$) and G_w ($0.2 \leq G_w \leq 0.6$). In all numerical computations Pr has been taken as 0.72. The edge of the boundary layer η_∞ is taken between 4 and 6 depending on the values of parameters. In order to verify the correctness of the procedure, solutions have been obtained for the non-similar incompressible flow cases by substituting $Pr = 1$ and $M_\infty = A = \theta = G_w = 0$ [$G = (T - T_w)/(T_\infty - T_w)$] to compare the skin friction and heat transfer parameters ($(F_\eta)_w$, $(S_\eta)_w = (G_\eta)_w$) with those obtained by using the differential-difference method [24, 25] and finite difference method [26]. The heat transfer result ($(G_\eta)_w$) has been compared with the experimental results [27]. The results are found to be in good agreement. The results, corresponding to $\xi = \bar{x} = 0$ in the present non-similar case, have been compared with the self-similar results obtained by Dewey and Gross [1], and found them in excellent agreement (these differ only in the fourth decimal place). We have also compared our results for zero yaw angle (i.e., for $\theta = 0$) with the steady state results of Vasantha and Nath [28] who studied the unsteady non-similar compressible boundary layer flow over a cylinder without mass transfer. The results are found to be in excellent agreement. Comparison of the results for zero yaw angle (i.e., for $\theta = 0$) is also made with the results of Roy and Nath [13] who studied recently the effect of non-uniform injection/suction combinations in a slot on a steady non-similar compressible boundary layer flow over a cylinder. The results are found to be in excellent agreement with the present results. Further, the comparison of the results is done with the most recent results of Roy [14] where the investigation has been made to study the effect of non-uniform injection/suction combinations in a single slot on a steady non-similar compressible boundary layer flow over a yawed infinite cylinder, and the results are found in excellent agreement with the present results. Comparisons are shown in Figs. 2–4 and in Table 1.

Case I: Non-uniform multiple slot injection (or suction)

Figs. 5–7 show the effects of non-uniform multiple slot injection (or suction) parameter ($A < 0$ or $A > 0$) and \bar{x}_1, \bar{x}_2 , which fix the slots positions (i.e., the porous sections on the surface of the body) through which mass transfer are considered, on the skin friction and heat transfer parameters ($(F_\eta)_w$, $(S_\eta)_w$, $(G_\eta)_w$). In the case of multiple slot suction ($A > 0$) the skin friction and heat transfer parameters ($(F_\eta)_w$, $(S_\eta)_w$, $(G_\eta)_w$) increase as the first slot begins and attain their maximum values before the trailing edge of the

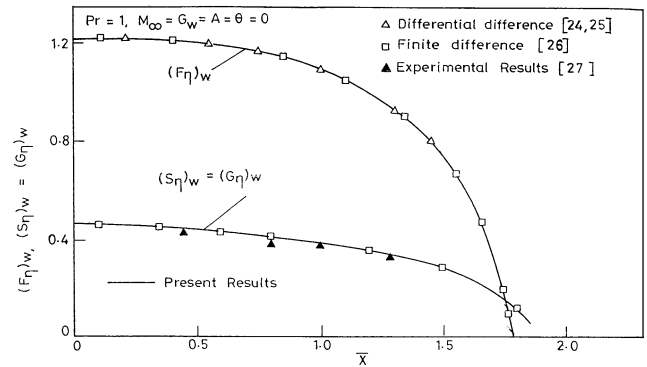


Fig. 2. Comparison of $(F_\eta)_w$ and $(S_\eta)_w = (G_\eta)_w$ with those obtained by other methods.

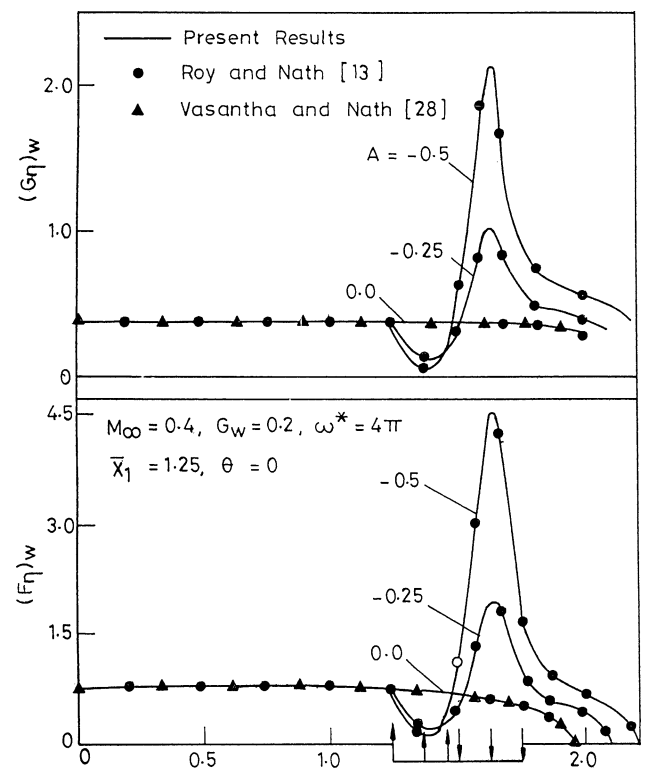


Fig. 3. Comparison of $(F_\eta)_w$ and $(G_\eta)_w$.

first slot. Next, $(F_\eta)_w$, $(S_\eta)_w$ and $(G_\eta)_w$ decrease from their maximum values at the trailing edge of the first slot. Similar variations of skin friction and heat transfer parameters ($(F_\eta)_w$, $(S_\eta)_w$, $(G_\eta)_w$) are also observed in the second slot, and finally beyond the trailing edge of the second slot, $(F_\eta)_w$ reaches zero but $(S_\eta)_w$ and $(G_\eta)_w$ remain finite (Fig. 5). This implies that an ordinary separation occurs at this point. For the problem under consideration, the singular separation has not been encountered (i.e., for no value of \bar{x} , $(F_\eta)_w = (S_\eta)_w = 0$ simultaneously). The above results hold good whatever may be the values of mass transfer parameter A . Hence in subsequent discussion the word separation denotes only the ordinary separation. The results indicate that the effect of non-uniform multiple slot suction ($A > 0$) is to move the point of separation downstream, i.e., it delays the

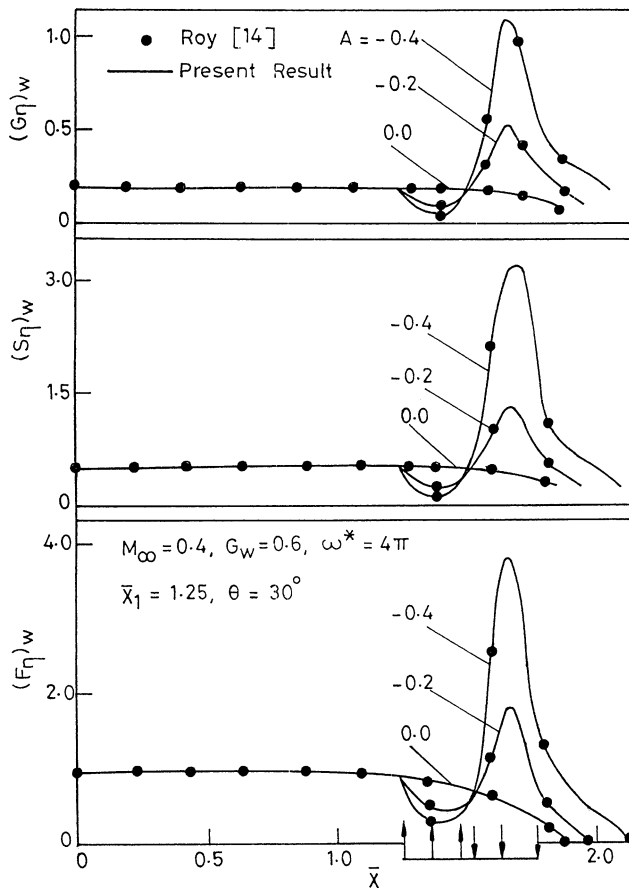


Fig. 4. Comparison of $(F_\eta)_w$, $(S_\eta)_w$ and $(G_\eta)_w$.

Table 1

Comparison of skin friction and heat transfer parameters with those tabulated by Dewey and Gross [1] for $\beta = 0.5$, $Pr = 1$, $A = \xi = \bar{x} = 0$

G_w	$E \sin^2 \theta$	Present results		Dewey and Gross [1]	
		$(F_\eta)_w$	$(S_\eta)_w = (G_\eta)_w$	$(F_\eta)_w$	$(S_\eta)_w = (G_\eta)_w$
0	0.3750	0.6439	0.5071	0.6438	0.5070
0	0.6667	0.7811	0.5330	0.7812	0.5328
0	0.8461	1.0892	0.5829	1.0890	0.5828
0	0.9000	1.3652	0.6213	1.3650	0.6211
0.5	0.3750	0.9169	0.5411	0.9167	0.5410
0.5	0.6667	1.2483	0.5835	1.2480	0.5833
0.5	0.8461	1.9663	0.6578	1.9660	0.6577
0.5	0.9000	2.6004	0.7115	2.6000	0.7113

separation but the non-uniform injection ($A < 0$) through multiple slots on the body surface has the reverse effect as shown in Fig. 7. Moreover, the multiple slot suction ($A > 0$) is found to be more effective in delaying the separation as compared to the single slot suction ($A > 0$). To be more specific, for $G_w = 0.2$ (Fig. 5), the point of separation moves downstream approximately by 8% and 15% for single slot suction and multiple slot suction, respectively, when the rate of suction has the fixed value $A = 0.25$. It is noted in Fig. 6 that if we move the locations of the slots downstream, the point of separation also moves downstream, (i.e., it delays

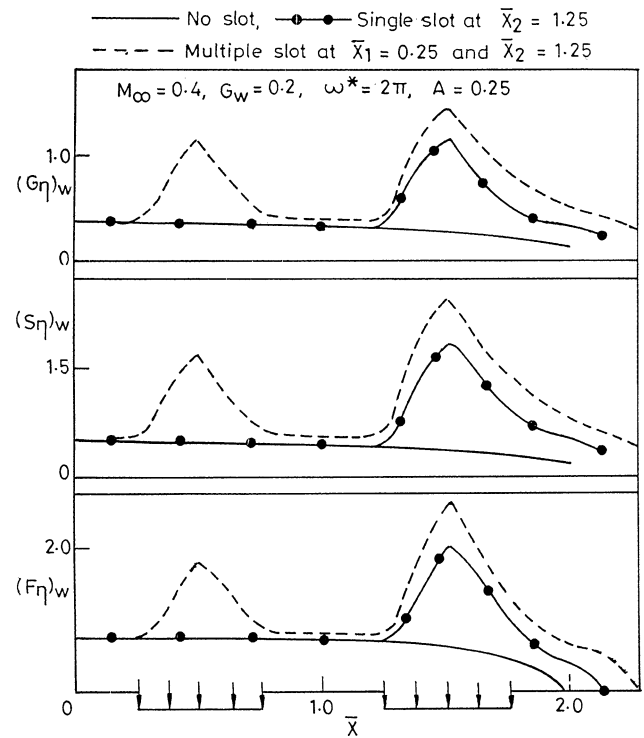


Fig. 5. Effect of suction ($A > 0$) on $(F_\eta)_w$, $(S_\eta)_w$ and $(G_\eta)_w$.

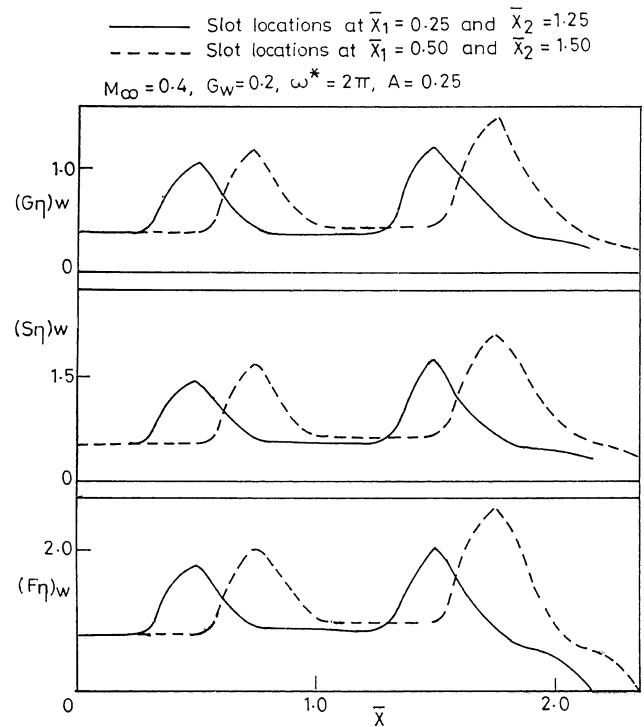


Fig. 6. Slot positions (\bar{x}_1, \bar{x}_2) variation effect on $(F_\eta)_w$, $(S_\eta)_w$ and $(G_\eta)_w$. (Slot locations are not shown in this figure.)

the separation). Thus, separation can be delayed by non-uniform multiple slot suction ($A > 0$) and also by moving the slots down stream.

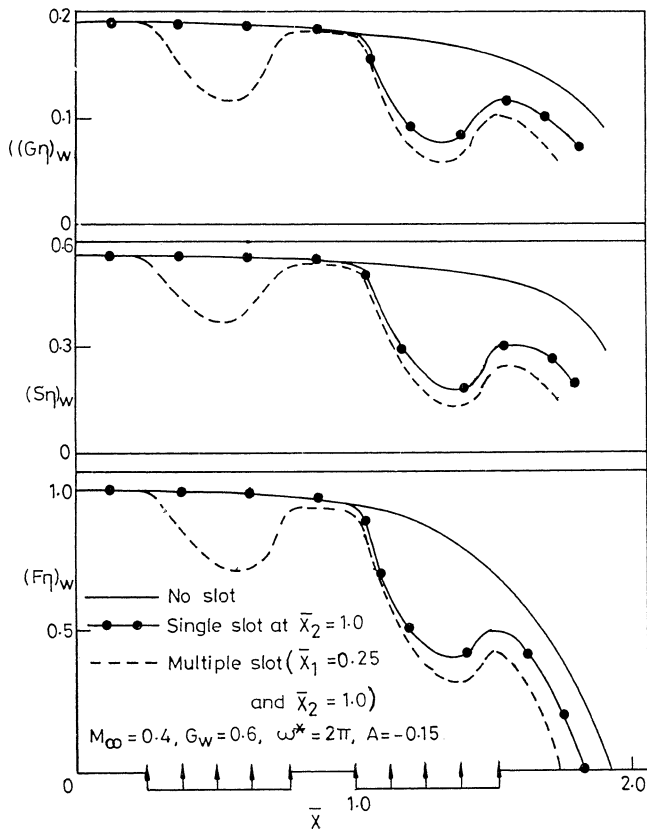


Fig. 7. Effect of injection ($A < 0$) on $(F_\eta)_w$, $(S_\eta)_w$ and $(G_\eta)_w$.

Effects of the total enthalpy at the wall (G_w) and the free stream Mach number (M_∞) on the skin friction and heat transfer parameters ($(F_\eta)_w$, $(S_\eta)_w$, $(G_\eta)_w$) are shown in Figs. 8 and 9. For a fixed M_∞ , an increase in total enthalpy at the wall (G_w) enhances the skin friction parameters ($(F_\eta)_w$, $(S_\eta)_w$) and also moves the separation point upstream. But, the heat transfer parameter ($(G_\eta)_w$) decreases with the increase of the total enthalpy at the wall (G_w). When wall temperature is increased, fluid near the wall becomes rarer. This results in a reduction in the skin friction at the wall causing the separation to occur earlier. The effect of decreasing M_∞ results in slight reduction in the values of $(F_\eta)_w$ and $(S_\eta)_w$, and the separation is delayed. Similar effect observed by Davis and Walker [29], and more recently, by Roy and Nath [13] and Roy [14] for non-similar compressible boundary layer flows over two-dimensional body, axi-symmetric body and over yawed cylinder. It has also been found that the yaw angle θ has little effect on the point of separation. In particular, the variations in the values of skin friction parameter ($(F_\eta)_w$) are within 1% for different values of θ ($0 \leq \theta \leq 45^\circ$) and the results are not presented here to limit the number of figures.

Case II: Non-uniform total enthalpy at the wall

The effect of non-uniform total enthalpy at the wall (i.e., the effect of cooling or heating in the slots at the wall along the streamwise direction) on the skin friction and

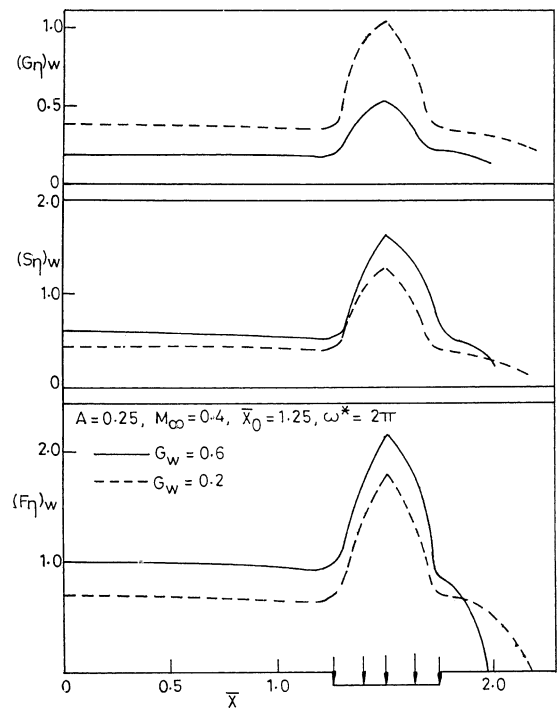


Fig. 8. Effect of G_w on $(F_\eta)_w$, $(S_\eta)_w$ and $(G_\eta)_w$.

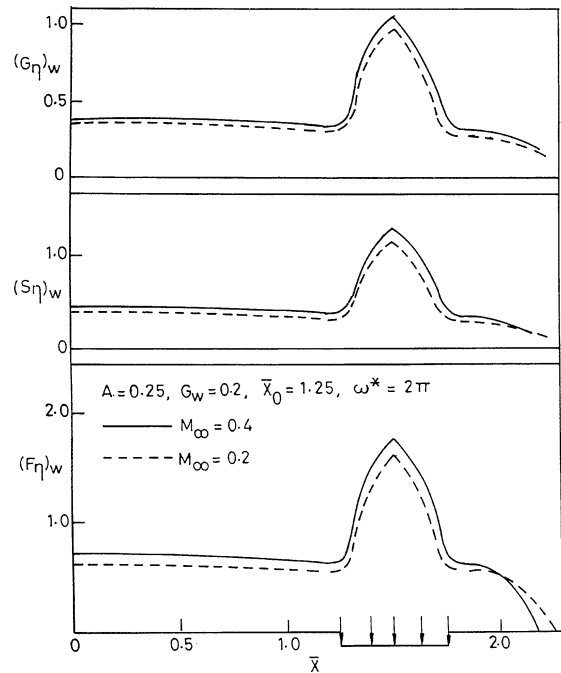


Fig. 9. Effect of M_∞ on $(F_\eta)_w$, $(S_\eta)_w$ and $(G_\eta)_w$.

heat transfer parameters ($(F_\eta)_w$, $(S_\eta)_w$, $(G_\eta)_w$) is shown in Fig. 10. The heat transfer parameter $(G_\eta)_w$ increases due to the wall cooling in the slots (Fig. 10), but decreases when there are wall heating in the slots (not shown to reduce the number of figures). The variation of the heat transfer parameter $(G_\eta)_w$ is strongly affected by the variation of the total enthalpy at the wall whereas the skin friction

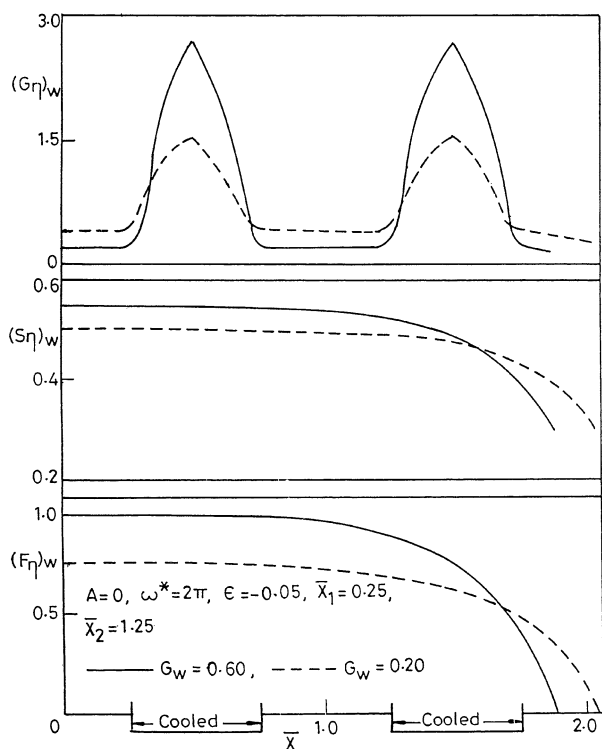


Fig. 10. Effect of wall cooling (in slots) on $(F_\eta)_w$, $(S_\eta)_w$ and $(G_\eta)_w$.

parameters $(F_\eta)_w$ and $(S_\eta)_w$ are very little affected by it (it is indistinguishable in this scale in Fig. 10) because the heat transfer parameter is more sensitive to the change in the total enthalpy at the wall than the skin friction parameters.

4. Conclusions

The results indicate that the separation can be delayed by non-uniform multiple slot suction and also by moving the slots downstream but the non-uniform multiple slot injection has the reverse effect. Moreover, the multiple slot suction is found to be more effective in delaying the separation as compared to the single slot suction. The increase of Mach number shifts the point of separation upstream due to the increase in the adverse pressure gradient. The increase of total enthalpy at the wall causes the separation to occur earlier while cooling delays it. The non-uniform total enthalpy at the wall (i.e., the cooling or heating of the wall in the slots) along the streamwise co-ordinate has very little effect on the skin frictions and thus on the point of separation. Also, the yaw angle has very little effect on the location of the point of separation.

References

- [1] C.F. Dewey, J.F. Gross, Exact similar solutions of the laminar boundary layer equations, in: *Advances in Heat Transfer*, Vol. 4, Academic Press, New York, 1967, pp. 317–446.
- [2] E.C. Maskell, Flow separation in three-dimensions, Royal Aircraft Establishment Rep. Aero. 2565, Farnborough, England, 1955.
- [3] T. Cebeci, A.K. Khattab, K. Stewartson, Three-dimensional laminar boundary layers and the OK of accessibility, *J. Fluid Mech.* 107 (1981) 57–87.
- [4] F.T. Smith, Steady and unsteady boundary layer separation, *Ann. Rev. Fluid Mech.* 18 (1986) 197–220.
- [5] J.C.Y. Koh, J.P. Hartnett, Skin friction and heat transfer for incompressible laminar flow over porous wedges with suction and variable wall temperature, *Internat. J. Heat Mass Transfer* 2 (1961) 185–198.
- [6] D.B. Spalding, H.L. Evans, Mass Transfer through laminar boundary layers, *Internat. J. Heat Mass Transfer* 2 (1961) 199–221.
- [7] M. Zamir, A.D. Young, Similar and asymptotic solutions of the incompressible laminar boundary layer equations with suction, *Aero Quart.* 18 (1967) 103–120.
- [8] F.T. Smith, K. Stewartson, On slot injection into a supersonic laminar boundary layer, *Proc. Roy. Soc. London A* 332 (1973) 1–22.
- [9] M.J. Werle, Supersonic laminar boundary layer separation by slot injection, *AIAA J.* 17 (1979) 160–167.
- [10] M. Napolitano, Numerical study of strong slot injection into a supersonic laminar boundary layer, *AIAA J.* 18 (1980) 72–77.
- [11] M. Napolitano, R.E. Messick, On strong slot injection into a subsonic laminar boundary layer, *Comput. Fluids* 8 (1980) 199–212.
- [12] N. Riley, Non-uniform slot injection into a laminar boundary layers, *J. Engrg. Math.* 15 (1981) 299–314.
- [13] S. Roy, G. Nath, Non-uniform slot injection (suction) or wall enthalpy into a steady nonsimilar compressible laminar boundary layers, *Acta Mech.* 103 (1994) 45–63.
- [14] S. Roy, Non-uniform slot injection (suction) into a compressible flow, *Acta Mech.* 139 (2000) 43–56.
- [15] A. Wortman, H. Ziegler, G. Soo-Hoo, Convective heat transfer at general three-dimensional stagnation points, *Internat. J. Heat Mass Transfer* 14 (1971) 149–152.
- [16] A.B. Cambel, *Plasma Physics and Magneto Fluid Mechanics*, McGraw-Hill, New York, 1963.
- [17] H. Schlichting, *Boundary Layer Theory*, 7th Edition, McGraw-Hill, New York, 1979.
- [18] R. Krishnaswamy, G. Nath, Compressible laminar boundary layers on a yawed infinite cylinder, *Indian J. Technol.* 21 (1983) 43–48.
- [19] S.I. Pai, *Introduction to the Theory of Compressible Flow*, Van Nostrand, New York, 1958.
- [20] C.F. Carrier, C.E. Pearson, *Partial Differential Equations Theory and Technique*, Academic Press, New York, 1976, pp. 134–139.
- [21] W.J. Minkowycz, E.M. Sparrow, G.E. Schneider, R.H. Pletcher, in: *Handbook of Numerical Heat Transfer*, Wiley, New York, 1988, pp. 140–144.
- [22] K. Inouye, A. Tate, Finite difference version of quasi-linearization applied to boundary layer equations, *AIAA J.* 12 (1974) 558–560.
- [23] R.S. Varga, *Matrix Iterative Analysis*, Prentice-Hall, New York, 2000.
- [24] A.M.O. Smith, D.W. Clutter, Solutions of incompressible laminar boundary layer equations, *AIAA J.* 1 (1963) 2062–2071.
- [25] A.M.O. Smith, D.W. Clutter, Machine calculations of compressible laminar boundary layers, *AIAA J.* 3 (1965) 639–647.
- [26] B.J. Venkatachala, G. Nath, Nonsimilar laminar incompressible boundary layers with vectored mass transfer, *Proc. Indian Acad. Sci. (Engrg. Sci.)* 3 (1980) 129–142.
- [27] E. Schmidt, L. Wenner, Wärmeabgabe über den Umfang eines angeblasenen geheizten Zylinders, *NACA TM* 1050, 1943.
- [28] R. Vasantha, G. Nath, Unsteady non-similar laminar compressible boundary layer flows over two dimensional and axi-symmetric bodies, *Acta Mech.* 57 (1985) 215–231.
- [29] T. Davis, G. Walker, On solution of the compressible laminar boundary layer equations and their behaviour near separation, *J. Fluid Mech.* 80 (1977) 279–292.